CMLS, Cell. Mol. Life Sci. 57 (2000) 871–883
1420-682X/00/060871-13 $ 1.50 + 0.20/0

CMLS Cellular and Molecular Life Sciences

Review

The plasma membrane proton-translocating ATPase

G. A. Scarborough

Department of Pharmacology, School of Medicine, Campus Box # 7365 Jones Building, University of North Carolina at Chapel Hill, Chapel Hill (North Carolina 27599, USA), Fax + 1 919 966 5640, e-mail: gas@med.unc.edu

Received 4 November 1999; received after revision 10 January 2000; accepted 13 January 2000

Abstract. Living cells require membranes and membrane transporters for the maintenance of life. After decades of biochemical scrutiny, the structures and molecular mechanisms by which membrane transporters catalyze transmembrane solute movements are beginning to be understood. The plasma membrane proton-translocating adenosine triphosphatase (ATPase) is an archetype of the P-type ATPase family of membrane transporters, which are important in a wide variety of cellular processes. The H^+-ATPase has been crystallized and its structure determined to a resolution of 8 Å in the membrane plane. When considered together with the large body of biochemical information that has been accumulated for this transporter, and for enzymes in general, this new structural information is providing tantalizing insights regarding the molecular mechanism of active ion transport catalyzed by this enzyme.

Key words. Membrane transport; membrane protein crystallization; P-type ATPases; proton pump; membrane protein structure; conformational changes; molecular dynamics.

Introduction

All living cells are surrounded by a hydrophobic lipid and protein layer known as the cell plasma membrane. More evolutionarily advanced cells contain, in addition to their plasma membrane, numerous intracellular membranes known as cell organelles. The primary function of all of these membranes is to regulate the transmembrane flow of a variety of ions, nutrients and other small and larger hydrophilic molecules, which are normally unable to penetrate the membrane. This makes possible the control of the chemical composition of the various membranous compartments, and the ability to control regional cellular chemical composition in this manner sufficiently defines the living state.

The molecular mechanisms by which polar solutes are made able to permeate hydrophobic lipid membranes have fascinated biological scientists for a century, ever since Overton established the existence of the cell plasma membrane [1]. Decades of intense biochemical scrutiny have provided a reasonably complete categorization of the various membrane permeation systems extant in nature, and the more recent explosion of information regarding genome sequences throughout biology has rounded out the list almost completely. The major categories of membrane proteins involved in transmembrane solute permeation now known include the bacterial porins [2], bacterio- and halorhodopsin [3], the phosphoenolpyruvate-dependent sugar phosphotransferase systems [4], the ion channels [5–7], the aquaporins [8], the connexins [9], the redox-coupled proton pumps [10], the facilitative and ion-coupled secondary transporters [11], the F- and V-type ion-translocating adenosine triphosphatases (ATPases) [12, 13], the P-type ion-translocating ATPases [14] and the ABC transporter family [15].

With a more or less complete inventory of nature's various membrane permeation systems in hand, the primary goals for the future are to understand how they work at the molecular and atomic levels of dimensions. Progress in this regard has been slow due to the dearth of information regarding the structures of membrane transporters and channels. But this situation is beginning to change, with spectacular structure determinations for several classes of membrane permeation systems in the last few years. X-ray and electron crystallographic analyses have recently elucidated the structures of bacteriorhodopsin [16–20], several porins [21–25] and related β-barrel proteins [26, 27], cytochrome oxidase [28, 29], cytochrome bc1 complex [30, 31], F1-H^+-ATPase [32, 33] and two different ion channels [34, 35]. In each of these cases, after the structure was seen, solid insight into the molecular mechanism emerged. Structure-based site-directed mutagenesis is now being applied to these systems, and an understanding of their molecular mechanisms is rapidly growing.

Whereas this recent progress is indeed stunning and satisfying, much remains to be done in the membrane transport field. Little is yet known about the atomic structures and hence mechanisms of the majority of membrane permeation systems that are known, including the sugar phosphotransferases, the aquaporins and connexins, the facilitative and ion-coupled secondary transporters, the complete F1FO ATPase complex, the V- and P-type ATPases and the ABC transporters.

The membrane transporter of primary interest in my laboratory is the proton-translocating ATPase from the plasma membrane of *Neurospora crassa*, which is an archetype of the P-type ATPase family of ion-translocating ATPases [14, 36]. This is a major family of ion-translocating ATPases in eukaryotic cells, which comprises about 80 members from all parts of the evolutionary tree [14]. These transporters are involved in a variety of cellular processes, including absorption, secretion, transmembrane signalling, nerve impulse transmission, excitation/contraction coupling, and growth and differentiation. The P-type ATPases are so named for the participation of a high-energy aspartyl-phosphoryl-enzyme intermediate in their catalytic cycle [36]. The aspartate phosphorylation occurs in a highly conserved asp-lys-thr-gly sequence in the amino-terminal half of the $\sim$100-kDa polypeptide chains of these enzymes, and is undoubtedly involved in the molecular mechanism of ATP hydrolysis-driven ion transport catalyzed by these enzymes. In a manner as yet unknown, the aspartate phosphorylation and dephosphorylation reactions are intimately coupled with the ion-translocation reactions, efficiently transducing the chemical energy of ATP hydrolysis into transmembrane electrochemical ion gradients. With the plasma membrane H^+-ATPase as our experimental object, our primary goal for many years now has been an elucidation of the molecular mechanism by which the P-type ATPases do this. In this article, our progress toward this ultimate end is reviewed.

Discovery of the H^+-ATPase

Electrophysiological experiments performed more than 30 years ago demonstrated that the plasma membrane of *Neurospora* generates and maintains a transmembrane electrical potential difference in excess of 200 mV, outside positive [37]. Subsequent studies correlated the membrane potential with intracellular ATP levels and extracellular acidification, and from these studies the idea of an electrogenic, proton-translocating ATPase in the fungal plasma membrane emerged [38]. Upon the development of a procedure for confidently isolating *Neurospora* plasma membranes [39], it could be demonstrated conclusively that a plasma membrane ATPase does exist, and studies of its biochemical properties subsequently ensued [40]. Shortly thereafter, in studies with isolated, everted plasma membrane vesicles, it was shown that the ATPase is indeed an electrogenic pump [41], and in a following study, the identity of the translocated ion as H^+ was clearly established [42]. Concomitantly, the hydrolytic moiety of the H^+-ATPase was identified as a polypeptide with a molecular mass of about 100 kDa that is phosphorylated and dephosphorylated at a rate comparable to the overall rate of ATP hydrolysis catalyzed by the ATPase, establishing that the catalytic cycle of this proton pump involves a phosphoryl-enzyme intermediate [43]. The subsequent demonstration that the kinetically competent intermediate is an enzyme-bound phosphoryl-aspartate [44] made it clear that except for the fact that the fungal plasma membrane ATPase catalyzes electrogenic proton translocation, it is otherwise quite similar to the Na^+/K^+-, Ca^{2+}-, and H^+/K^+-translocating ATPases of animal cell membranes. The more recent availability of gene sequence information has borne this out, and in addition has included a great many other ATPases in the rather large P-type ATPase family [14].

Additional biochemical features and early structural studies of the H^+-ATPase

Detergent solubilization of the H^+-ATPase was problematic, but the detergent, lysolecithin, eventually proved to be quite effective for this purpose. A small-scale purification procedure for the lysolecithin-ATPase complex was developed [45], and a large-scale method for the facile isolation of 50–100-mg quantities of the ATPase was then devised [46, 47]. A procedure for reconstituting the purified ATPase in fully functional

form into artificial phospholipid vesicles was also worked out [48], and using this reconstituted system it was possible to demonstrate that the H^+-ATPase has no subunits other than the ATP hydrolytic subunit [48], and that one copy of the 100-kDa hydrolytic moiety alone is capable of efficient ATP-hydrolysis-driven proton translocation [49]. A high-yield yeast expression system for defining the function of key residues of the H^+-ATPase by site-directed mutagenesis was also developed [50].

The structure of the H^+-ATPase molecule has been probed by a variety of techniques. Biochemical studies have shown that the H^+-ATPase is a hexamer as isolated [51] and that the functional properties of this form of the enzyme are the same as those of the ATPase in its monomeric membrane-bound state [52]. An accurate estimation of the secondary structure compostition of the ATPase by circular dichroism was made possible by the unique, largely lipid- and detergent-free nature of the purified hexameric ATPase preparation [52], and importantly, an essentially identical secondary structure composition was obtained for the ATPase in its membrane-bound state by infrared attenuated total reflection spectroscopy [53]. Thus, the secondary structure elements that the ATPase comprises are reasonably certain. Protein chemistry procedures for fragmenting the ATPase molecule by trypsinolysis and purifying most of the numerous hydrophilic and hydrophobic fragments produced were developed [54, 55], and with this technology and the purified, reconstituted ATPase proteoliposomes, the transmembrane topography of virtually all of the 919 amino acid residues in the H^+-ATPase molecule was defined [56–59]. The cysteine chemistry of the ATPase was also defined by protein chemistry techniques [60]. Figure 1 shows the H^+-ATPase folding model that was generated from these results. By this time, it was reasonably clear that this transport molecule comprises a large cytoplasmic region with both the N- and C-termini, a presumably α-helical membrane-embedded domain, and a minimal loop region exposed to the extracellular side of the membrane. Since the discovery of the H^+-ATPase, a large amount of information has accumulated about it and the closely related yeast and plant plasma membrane H^+-ATPases. Summaries of the large amount of work on these enzymes can be found in numerous reviews [61–66].

Crystallization of the H^+-ATPase

The fundamental advance that made possible much of our recent progress with the H^+-ATPase was the development of a new approach to the crystallization of the detergent complexes of integral membrane proteins, utilizing the ATPase as our first experimental object [67]. The standard approach to crystallizing soluble proteins involves an empirical search for an appropriate precipitant that will render the protein solution mildly supersaturated, from which crystals will form as protein-protein interactions replace solvent-protein interactions. However, when this approach is tried with detergent complexes of membrane proteins, crystals are rarely produced. It seemed possible that the chimeric nature of membrane protein-detergent complexes is a fundamental problem that often precludes their crystallization using the standard approach. That is, detergent complexes of integral membrane proteins are chimeras, with conventional protein surfaces made up of the standard polypeptide functional groups, and with a detergent micellar collar surrounding the part of the protein normally embedded in the lipid bilayer. And whereas it should be relatively straightforward to find conditions empirically that render the protein part of a membrane

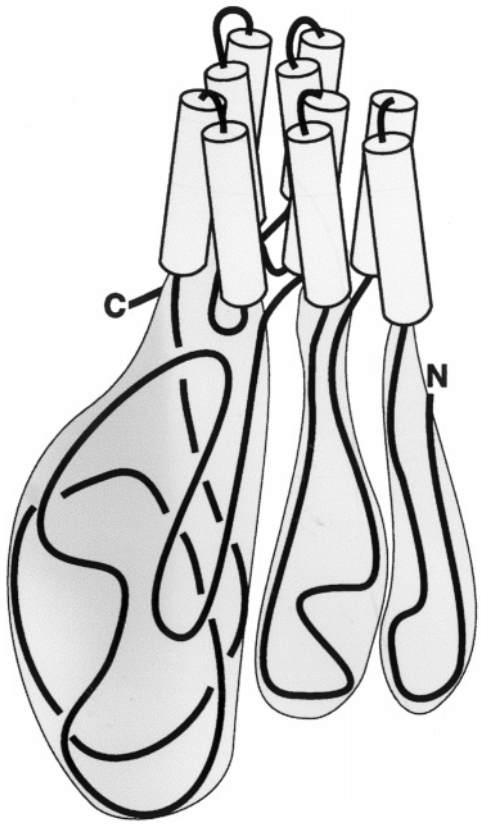

Figure 1. Original folding model of the plasma membrane proton pump based on hydropathy analysis, tryptic cleavage experiments and other biochemical approaches. The H^+-ATPase comprises a large cytoplasmic region with both the N- and C-termini, a transmembrane helix region and a helix-connecting loop region on the exocytoplasmic side of the molecule. The cylinders represent the membrane-embedded domain of the molecule.

protein-detergent complex mildly supersaturated, it is unlikely that those conditions would also render the detergent micellar collar suitably insoluble. It was thus reasoned that a key to crystallizing membrane-protein detergent complexes may be the attainment of conditions in which the protein surfaces of the chimera are moderately supersaturated, encouraging protein-protein interactions, and in which the the detergent micellar collar is also at or near its solubility limit so that detergent-detergent interactions are promoted as well. These considerations suggested that the conventional random search for suitable precipitants was not likely to be a very successful approach for crystallizing the ATPase, and numerous unsuccessful attempts to crystallize it in this way lent support to this notion.

With some confidence that the above hypothesis might be valid, it was therefore decided to approach the problem more systematically in an attempt to find conditions in which the extent of supersaturation of the protein surfaces of the ATPase and the detergent micellar collar were properly matched. Preliminary experiments had indicated that the ATPase is most stable when the detergent used to maintain its solubility is dodecylmaltoside (DDM). The first step was thus to screen a variety of commonly used protein precipitants for those that were able to induce the aggregation of pure DDM micelles. The concentration at which any precipitant induced DDM micellar aggregation was hoped to be close to the concentration at which it might induce insolubility of the detergent micellar collar of the DDM-ATPase complex. Of the nine precipitants tried, seven, all polyethylene glycols (PEGs), were able to induce DDM micelle insolubility. The seven PEGs were then tested for their effect on the solubility of the DDM-ATPase complex, at a concentration slightly below that necessary to induce DDM micellar aggregation. Three of the PEGs caused extensive precipitation of the ATPase at this concentration and were therefore shelved. The other four PEGs did not induce precipitation at the concentration employed and were subsequently used at this concentration for crystallization trials in which the protein concentration was varied. Encouragingly, crystalline plates of the ATPase were obtained for each of the four PEGs tried, indicating that the overall approach may be valid. Unfortunately, the crystals obtained were visibly flawed, suggesting that the proper balance of protein surface and DDM micelle insolubility had not yet been reached. The ionic strength of the crystallization trials was then raised, which was known from other experiments to render the protein surfaces of the ATPase less soluble while having no effect on the DDM micellar aggregation point. For one of the PEGs, PEG 4000, this brought on a new, well-formed hexagonal crystal habit. Subsequent optimization of the initial conditions has yielded large, single, hexagonal three-dimensional (3D) crystals of the H^+-ATPase up to about $0.4 \times 0.4 \times 0.15$ mm in size that occasionally diffract X-rays to better than 4 Å resolution using synchrotron radiation. An X-ray diffraction analysis of the H^+-ATPase crystals is in progress.

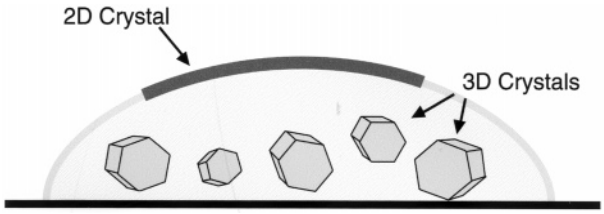

Figure 2. Precipitant-induced surface crystallization. H^+-ATPase crystallization drops contain 3D microcrystals that grow in the drops and 2D crystals that grow at the air-water interface.

Two-dimensional (2D) crystals of the H^+-ATPase

Electron microscopy of 3D crystals has often been used to obtain intermediate-level resolution images of protein molecules, and this information can sometimes aid in the interpretation of higher-resolution X-ray diffraction data [68]. For this reason, we decided to initiate an exploration of the H^+-ATPase crystals by electron microscopic techniques. To facilitate these studies, the ATPase crystallization procedure was adapted for the production of thin microcrystals of the enzyme [G. A. Scarborough, unpublished experiments]. In addition to providing microcrystals of the ATPase, these early studies clearly showed the predilection of the ATPase for crystallizing on surfaces, as crystals were found in large numbers growing on glass cover slips during light microscopy. In a subsequent electron microscopic investigation of the 3D microcrystals, it was then discovered that large, 2D crystals also grow in the microcrystallization drops at the air-water interface [69]. Conventional 2D crystallization of membrane proteins involves preparing mixtures containing the protein of interest and a suitable lipid, both solubilized by an appropriate detergent, after which the detergent is removed by dialysis or other means, and 2D crystals form as proteolipid sheets [70]. The precipitant-induced 2D surface crystals of the DDM complex of the H^+-ATPase thus represent an entirely new approach to obtaining 2D crystals of integral membrane proteins useful for structure analysis. Figure 2 shows a diagram of this crystallization system. Whereas 3D H^+-ATPase crystals grow in the drops, large 2D H^+-ATPase crystals readily grow on the surface of such drops. The 2D H^+-ATPase crystals

can be picked up by touching the surface of the drops with a carbon-coated electron microscope grid and can then be viewed by electron microscopy. Figure 3 shows negative stain images of the 2D H^+-ATPase crystals at the beginning of their formation and after the formation of a large 2D surface crystal. The small circular protomeric units are H^+-ATPase hexamers.

Structure of the H^+-ATPase

Our first step in the investigation of the H^+-ATPase structure using the surface crystals was an analysis of untilted specimens by electron cryomicroscopy [69]. Selected images were digitized, Fourier-transformed and processed as described [69]. The inverse Fourier transform of the first image processed yielded the 22 Å projection map shown in figure 4. The ringlike nature of the H^+-ATPase hexamers is clearly evident in the map. The unit cell is hexagonal with $a = b = 167$ Å. The individual monomers in projection are shaped like a boot. Further improvements in specimen preparation and merging of the data from several images yielded an improved projection map with a resolution extending to 10.3 Å [69].

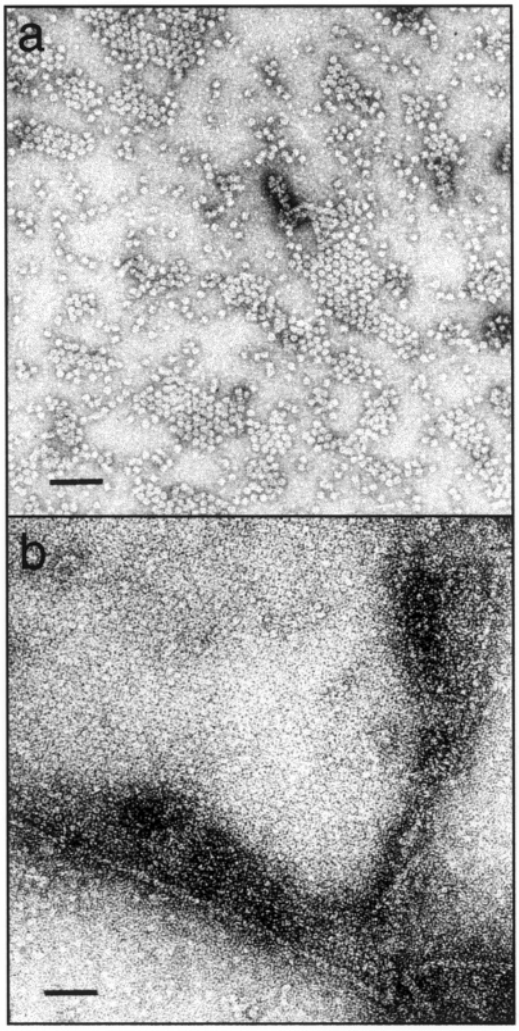

Figure 3. Electron micrographs of the precipitant-induced 2D H^+-ATPase surface crystals. The individual circular particles are H^+-ATPase hexamers, the fundamental crystallizing unit. (*a*) Incipient crystals are evident as small patches of hexamers coalescing into a hexagonal lattice. (*b*) Large single 2D surface crystals of the H^+-ATPase form at longer incubation times. The scale bars indicate 100 nm.

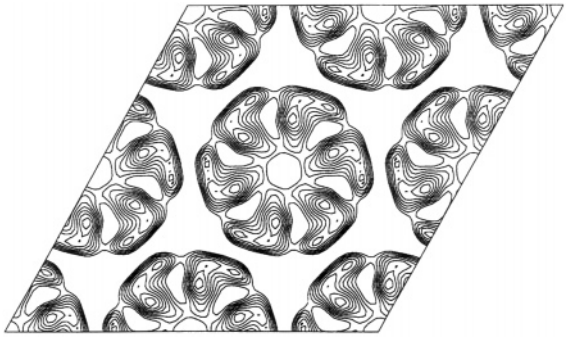

Figure 4. Projection map of the H^+-ATPase structure obtained by electron cryomicroscopy and image processing. The electron density distribution map was derived from an individual image at 22 Å resolution. The circular units are H^+-ATPase hexamers approximately 160 Å in diameter. The individual H^+-ATPase monomers in projection are shaped like a boot.

The 2D H^+-ATPase crystals that grow at the air-water interface are quite fragile, and the major problem we experienced with them is their tendency to crack during the preparation of specimens for cryoelectron crystallography. Experiments were thus performed to develop a suitable procedure for specimen preparation. The results of these experiments led to a simple but effective procedure in which the 2D crystals are grown directly on carbon-coated electron microscope grids and then immediately frozen in liquid ethane. This eliminated the need to pick the crystals off of the surface of the crystallization drops before freezing and greatly diminished the cracking problem [71].

With a suitable procedure for obtaining 2D H^+-ATPase crystals physically stable enough to permit the reproducible generation of cryoelectron microscope images suitable for analysis, numerous images were processed. A tilt series was then carried out, and the data were successfully merged, which produced a 3D density map of the H^+-ATPase crystals at a resolution of 8 Å in the membrane plane [72].

Figure 5a shows a cross-section of the H^+-ATPase structure map cut perpendicular to the 2D crystal and membrane plane. The crystals consist of two layers of

H^+-ATPase hexamers, separated by a narrow region of low density, and related to one another by twofold symmetry. Within each layer, regions of tightly packed rod-shaped densities, characteristic of transmembrane α-helices at this level of resolution and perpendicular to the membrane plane, define the membrane-spanning domain of the H^+-ATPase (arrow 1). The large cytoplasmic regions of the H^+-ATPase (arrow 2) extend from the membrane domains toward each of the 2D crystal surfaces. This view also shows the main interconnection between the layers (arrow 3), which occurs via loops of the polypeptide chain on the exocytoplasmic surface of the molecule. There are three of these contacts for each ATPase hexamer.

Figure 5b shows a section parallel to the crystal plane at the level of the membrane. The slice was made approximately through the region indicated by arrow 1 in figure 5a. This view shows a striking pattern of circular units tightly packed on a hexagonal lattice, each unit representing an H^+-ATPase hexamer. At this level of the map, the hexamers appear as two concentric rings with outer diameters of 115 and 165 Å, respectively. The inner ring comprises six sets of 10 transmembrane helices arranged in a ring around an apparent sixfold symmetry axis, representing the membrane domain of six ATPase monomers. Although the presence of transmembrane helices in the molecule was suspected, their existence, and their number, were conjectural until the structure was seen.

An unexpected largesse that emerged from the structure map is the clear-cut visualization of the organization of the detergent in the H^+-ATPase crystals. The outer rings seen in figure 5b are the DDM used in the H^+-ATPase crystallization system. Cross-sections of the detergent rings, indicated by the stars, can be seen in figure 5a just outside the transmembrane helix region of each hexamer. The detergent thus forms toroid rings around the normally membrane-embedded regions of six monomers of the H^+-ATPase hexamers, and these rings then bind side to side and probably also face to face in certain regions to form an organized detergent network in the crystals. Detergent-detergent interactions thus appear to provide a substantial contribution to the crystal-packing forces in the H^+-ATPase crystals.

Figure 5c shows a similar slice through the large cytoplasmic domain region that lies above the membrane region. The slice was made approximately through the region indicated by arrow 2 in figure 5a. It shows clearly that protein-protein crystal contacts occur in the cytoplasmic region as well. The predominant crystal contact in this region of the crystals is indicated by the arrow. Thus, another important piece of information that emerged from the structure is that the crystal contacts comprise both protein-protein and detergent-detergent

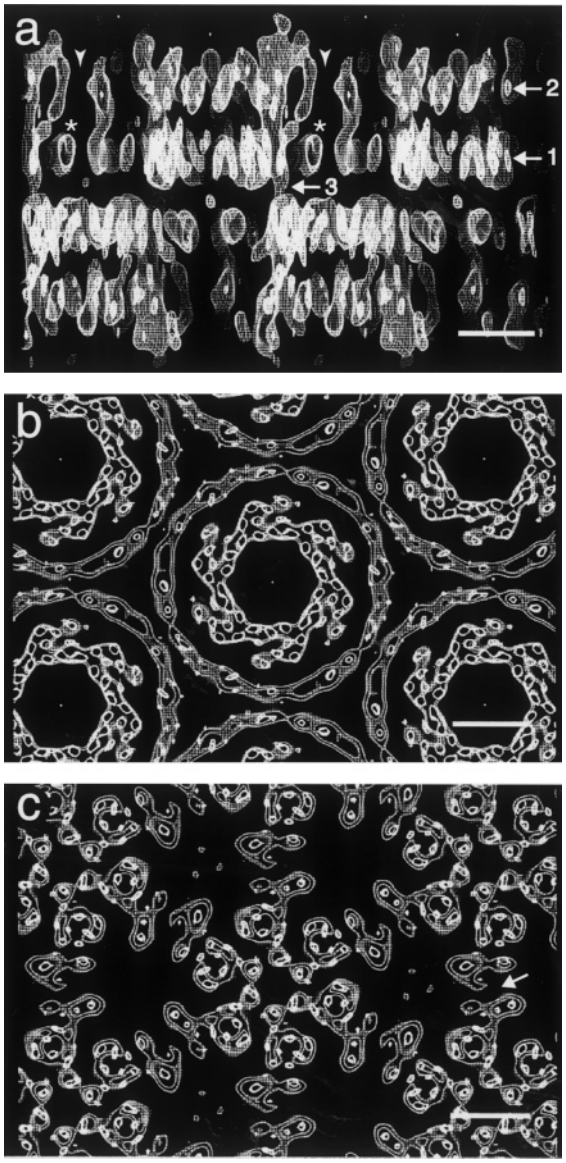

Figure 5. The H^+-ATPase structure map. Several views of the electron density distribution in the 2D H^+-ATPase crystals are shown. Panel *a* shows a cross-section of the map cut perpendicular to the 2D crystal plane, which is also the membrane plane. The vertical arrowheads delineate the density of a single ATPase hexamer. The crystals consist of two offset layers of ATPase hexamers separated by a narrow region of low density. Arrow 1 in panel *a* points to the membrane-embedded region of the ATPase in one of the layers. Arrow 2 in panel *a* points to the cytoplasmic region of the ATPase in the same layer. Arrow 3 points to the major protein-protein contact between the layers. The stars in panel *a* mark cross-sections of the detergent rings. Panel *b* shows a section of the map cut parallel to the crystal plane through one of the hexamer layers in the membrane-embedded region of the ATPase at a level indicated approximately by arrow 1 in panel *a*. Panel *c* shows a similar section cut through the map at a level indicated approximately by arrow 2 in panel *a*. The arrow in panel *c* indicates a major protein-protein contact in the ATPase crystal lattice. Scale bars, 5 nm. See text for additional details.

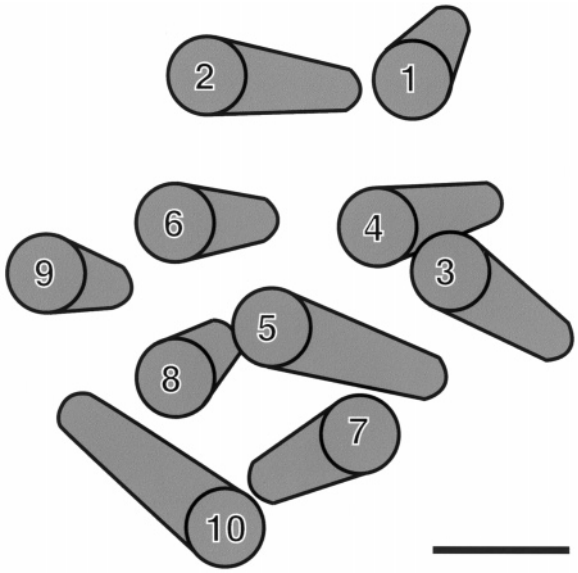

Figure 6. Drawing of the 10 transmembrane helices of an H^+-ATPase monomer viewed from the cytoplasmic side of the membrane. Each cylinder follows the density of a transmembrane helix in the structure map shown in figure 5. The helices are numbered according to their probable order in the linear sequence as described in the text. The scale bar indicates 1 nm.

interactions. As mentioned above, the original approach to obtaining the H^+-ATPase crystals recognized the possible importance of attaining a balance between the solubility of the protein surfaces of the H^+-ATPase molecule and the solubility of its detergent micellar collar surrounding the membrane-embedded region [67]. The clear-cut demonstration of both protein-protein and detergent-detergent interactions in the H^+-ATPase crystal structure lent gratifying credence to the validity of this concept and augurs that it might be useful for obtaining 2D and 3D crystals of other membrane proteins. In accord with this, the sparse matrix membrane protein crystallization protocols described by Song and Gouaux [73] are designed to maintain the conditions near the solubility limit of the detergent micelles.

Figure 6 shows a drawing of the transmembrane helix region of an H^+-ATPase monomer, viewed from the cytoplasm. The transmembrane helix region covers an area of about 30 Å by 40 Å and is 35–40 Å thick, as judged by the average extent of the membrane-spanning helices in the vertical direction. The 10 membrane-spanning helices are numbered according to their probable position in the polypeptide chain, based on as yet unpublished data from the laboratory of C. Toyoshima for the closely related Ca^{2+}-ATPase of sarcoplasmic reticulum. The helices are tightly packed, with center-to-center distances at the points of closest contact ranging from about 8 to 13 Å. None of them run exactly perpendicular to the membrane plane. Tilt angles of helices 1, 3, 6, 7, 8 and 9 range from ~5° to ~15°, whereas helices 2, 4, 5 and 10 are more highly tilted by ~16° to ~22°. Helices 5, 7, 8 and 10 appear to form a four-helix bundle with a pronounced right-handed twist. Helices 3, 4, 6 and 9 form a second layer on one side of the bundle, their orientation being similar to that of helices 5 and 8. Helices 1 and 2, which again have the same orientation, form a third layer. Most helices are essentially straight except helices 2 and 5, which are slightly curved. The apparent lengths of the individual membrane-spanning helices vary considerably, but they average about 35 Å long, as expected for membrane-spanning helices.

Figure 7 shows a surface-shaded representation of a single H^+-ATPase monomer, viewed along the membrane plane. As mentioned above, the monomer is the functional unit for this transporter [48, 49]. A lipid

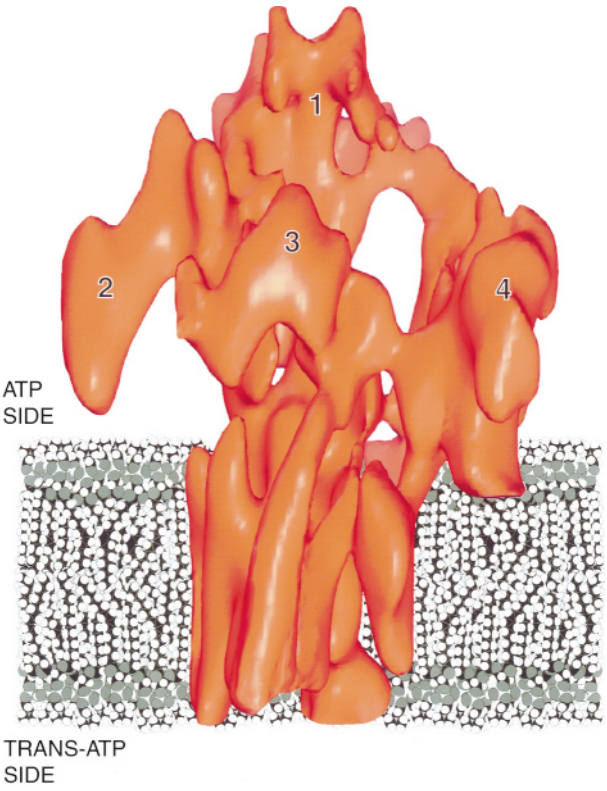

Figure 7. Surface-shaded representation of the structure of the plasma membrane H^+-ATPase. A phospholipid bilayer has been added to orient the molecule with respect to the membrane. The principal cytoplasmic domains are numbered 1–4. ATP side refers to the cytoplasmic side of the membrane, and trans-ATP side refers to the exocytoplasmic side of the membrane.

bilayer has been added to orient the molecule with respect to the membrane. The H^+-ATPase possesses a large portion on the cytoplasmic side of the membrane, a membrane sector that constitutes approximately one-fourth of the molecule, and a small extracellular portion. The similarity of the real H^+-ATPase structure to the folding model of figure 1 based upon our earlier biochemical studies is quite satisfying. Another important feature of the ATPase molecule revealed by the structure is the existence in the cytoplasmic region of several separate domains, numbered 1–4 in figure 7. Domain 1 is the largest, and it is separated from both domains 3 and 4 by deep clefts. Each of domains 1, 3, and 4 is connected to the membrane by extensions of the transmembrane helices. Domain 2 is an extension of domain 1 and is involved in the formation of the hexamers that form when the ATPase is isolated [51].

Conformational dynamics of the H^+-ATPase molecule

Early in our investigation of the H^+-ATPase, experiments carried out with isolated plasma membranes showed that the enzyme is protected against inhibition by mercurials or trypsin by its substrate, MgATP [40]. Subsequently, the differential sensitivity of the ATPase to tryptic degradation in the presence or absence of MgATP served in the identification of the hydrolytic moiety of the ATPase, and during these studies, it was noted that the potent ATPase inhibitor orthovanadate enhances the protective effects of MgATP against tryptic degradation [43]. It was also shown later that the combination of MgATP and vanadate confers stability to the ATPase during detergent solubilization and purification [45]. These various results strongly indicated that the ATPase undergoes significant conformational changes during its catalytic cycle, and because these conformational changes are almost certainly intimately related to the transport mechanism, they were investigated in more detail in a study of the effects of a variety of ATPase ligands and ligand combinations on the sensitivity of the ATPase to degradation by trypsin [74]. To summarize the results of these experiments, with no ligand present, the H^+-ATPase is rapidly degraded by trypsin to small fragments. In the presence of the nonhydrolyzable competitive inhibitor, MgADP, an $\sim$7.6-kDa piece is rapidly removed from the N-terminus, but further degradation of the resulting $\sim$92-kDa enzyme occurs much more slowly, suggesting that the H^+-ATPase changes its conformation upon binding its substrate. Importantly, in the presence of another nonhydrolyzable competitive inhibitor, Mg β,γ-methylene ATP, an $\sim$3.6-kDa piece is rapidly removed, again from the N-terminus, but further degradation of the resulting $\sim$96-kDa enzyme occurs much more slowly, suggesting that the enzyme assumes a different conformation when bound to Mg β,γ-methylene ATP, even though MgADP and Mg β,γ-methylene ATP are both competitive inhibitors of the H^+-ATPase. Finally, and perhaps most important, in the presence of Mg^{2+} and the potent inhibitor, vanadate, the tryptic degradation pattern is indistinguishable from that seen in the presence of Mg β,γ-methylene ATP.

The profound effects of the various ATPase ligands on the sensitivity of the H^+-ATPase molecule to trypsinolysis seemed to indicate that the ligand-induced conformational changes are quite extensive. However, ligand protection of only a few key amino acid residues could conceivably explain the results of these experiments. The ligand-induced ATPase conformational changes were thus further explored using attenuated total reflection Fourier transform infrared spectroscopy [53]. The results of these experiments clearly showed that the secondary structure components of the H^+-ATPase, i.e. α-helix, β-sheet, turns and random coil, do not change when the H^+-ATPase undergoes these ligand-induced conformational changes, in agreement with our earlier circular dichroism studies [52]. But importantly, the hydrogen/deuterium (H/D) exchange rates of roughly 175 surface amide linkages in the ATPase polypeptide chain out of a total of about 350 are drastically reduced as the ATPase proceeds from its unliganded conformation to its substrate binding conformation (i.e. bound to MgADP). Similarly, the H/D exchange rates of about 130 residues are reduced in the transition state of the enzyme dephosphorylation reaction (i.e. bound to Mg-vanadate in the presence of ATP). These results thus clearly indicate that the ligand-induced H^+-ATPase conformational changes are quite substantial.

It is important at this juncture to briefly discuss the transition state theory of enzyme catalysis and known modes of enzyme conformational dynamics, since they are essential for the interpretation of the above experimental results. There is general agreement that enzyme-catalyzed phosphoryl transfer reactions proceed via in-line, associative, SN2-type nucleophilic displacement reactions [75, 76]. In such a displacement reaction, when the incoming nucleophile and the leaving group are roughly the same distance from the phosphorus atom undergoing the substitution reaction, the system is said to be in the transition state. As pointed out by Pauling [77], and elaborated upon later by others [78–81], enzymes facilitate chemical reactions by binding most tightly to the transition state configuration of the reaction that they catalyze. In so doing, they stabilize the transition state and thus increase its relative concentration, which, according to the transition state theory of reaction rates [82], leads to rate enhancement because the transition state concentration is rate-determining. Implicit in this view of catalysis are numerous favorable

bonding interactions between enzyme functional groups and the transition state configuration of the chemical constituents undergoing the reaction, and the summation of these favorable bonding interactions would constitute a free energy well leading to the cessation of catalysis were it not for the extreme chemical instability of the transition state. It follows that if an enzyme comes in contact with a stable compound already having, or capable of readily assuming, the molecular configuration of the transition state, the enzyme will seize upon the so-called transition state analogue and be powerfully inhibited. This is what vanadate is thought to do to the enzymes that it strongly inhibits [83], presumably acting as a transition state analogue of the enzyme dephosphorylation reaction. As a related issue, if enzyme conformational changes are involved in optimizing enzyme-transition state complementarity [84], the tight binding of a transition state analogue will lock the enzyme in the transition state conformation.

Figure 8 shows this concept with a generalized phosphoryl-transfer enzyme. Most enzymes operate as shown in this figure. They have at least two domains separated by a cleft, they are open in the absence of substrate, and upon binding their substrates, they close by rigid body interdomain movements to envelop the reactants. In doing so, they stabilize the transition state of the reaction, as shown at the bottom for a phosphoryl transfer reaction. This is what orthovanadate looks like to the P-type ATPases. When the transition state decomposes, enzymes virtually always reopen and release their products in preparation for another round of catalysis. The conformational changes need not be as extensive as the example shows, but in the case of phosphoryl transfer enzymes, they have proved to be in all cases where they have been thoroughly studied.

When viewed within this general framework, the results of the abovementioned trypsinolysis and hydrogen/deuterium exchange experiments with the H^+-ATPase are readily interpreted, and an approximate outline of the events that take place during the catalytic can be formulated. In the absence of any of its ligands besides protons, the H^+-ATPase is in the open conformation shown in figure 7. In this state, the enzyme is readily degraded by trypsin to small fragments, and roughly 350 residues are exposed to the aqueous environment and available for rapid hydrogen/deuterium exchange. Upon the binding of MgADP, the ATPase undergoes a conformational change involving rigid body interdomain movements to a form that is much more compact, with the occlusion of 175 additional surface residues and a profound increase in resistance to trypsinolysis. This conformational change may be likened to the closing of the petals of a tulip, or perhaps a Venus's flytrap [85]. In this form, only a few residues at the N-terminus, specifically, those upstream from val74 [86], can be cleaved from the molecule by trypsin. Of course, MgADP is not a suitable substrate for driving transport due to its lack of a γ-phosphoryl group. When a γ-phosphoryl group is present, i.e. when the substrate is MgATP, the H^+-ATPase undergoes a similar, but distinguishably different conformational change con-

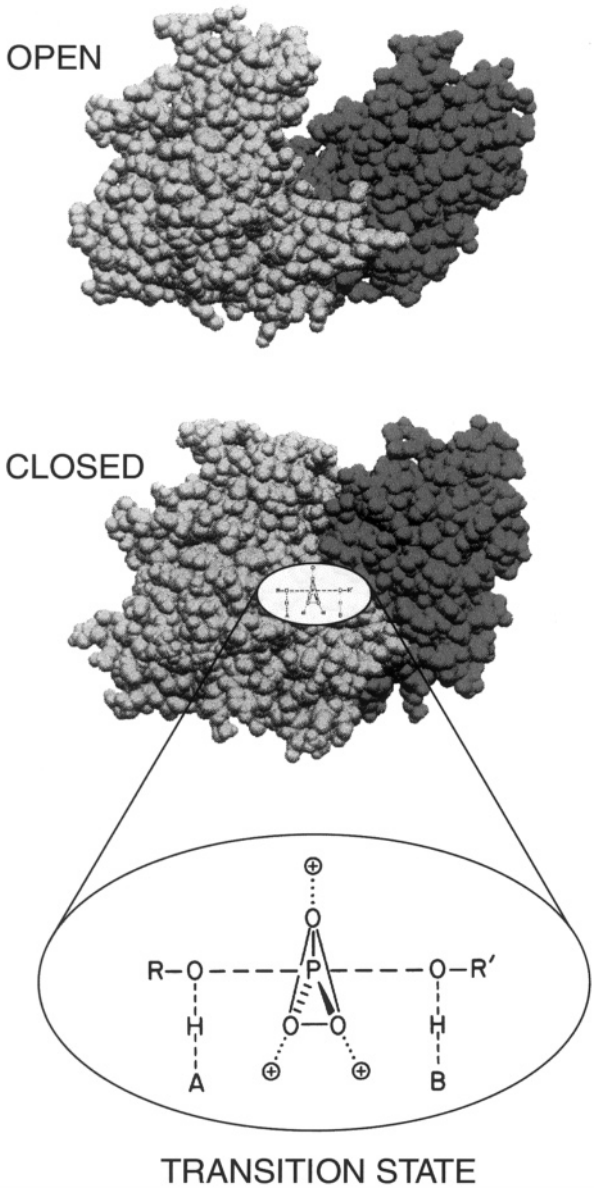

Figure 8. Enzyme catalysis by phosphoryl-transfer enzymes. The generalized phosphoryl-transfer enzyme is in an open conformation prior to substrate binding. Upon binding of its substrate, the enzyme undergoes a rigid-body interdomain movement with cleft closure in order to optimize transition state binding, which is the essence of enzyme catalysis. The transition state of a generalized phosphoryl-transfer reaction [76] is magnified at the bottom of the figure.

comitant with the formation of the transition state of the enzyme phosphorylation reaction. The form of the enzyme that results from these events can only be N-terminally cleaved by trypsin at lys36 [86], indicating that arg73 is occluded in addition to the other occluded trypsin-sensitive sites. This may indicate the involvement of residues between lys36 and val74 in the formation of the transition state of the enzyme phosphorylation reaction, which would be consistent with the facts that the enzyme cleaved at arg73 is inactive, whereas the enzyme cleaved at lys36 is fully functional [74, 86]. Mg β,γ-methylene ATP can lock the enzyme in this conformation because the complete enzyme transphosphorylation reaction cannot occur due to the stability of the β,γ-methylene bridge. When the substrate is MgATP, the transition state of the enzyme phosphorylation reaction breaks down with the formation of ADP and the aspartyl-phosphoryl-enzyme intermediate at asp378. The nature of the next few steps must remain, at present, unspecified. And whether or not the molecule reopens after the first transition state breaks down is unknown. But at some point, ADP debinds, and a water molecule approaches the phosphorus atom of the phosphorylated aspartate in preparation for the formation of the transition state of the enzyme dephosphorylation reaction. Upon the formation of the transition state of the enzyme dephosphorylation reaction, information is again available as to the conformation of the H^+-ATPase molecule. This is the conformation in which the enzyme is locked in the presence of Mg^{2+} plus orthovanadate. The conformation of the enzyme in this second transition state appears to be similar to the conformation of the enzyme in the first transition state, because the tryptic degradation patterns of the enzyme in the two transition state conformations are so similar, with the occlusion of arg73 and the other trypsin-sensitive sites that are available in the open form. The hydrogen/deuterium exchange data show directly that the enzyme is relatively closed in this conformation, with the occlusion of roughly 130 of the 350 residues available in the open conformation. This suggests that only a minimum amount of atomic movement may occur as the enzyme proceeds from the first transition state to the second. The reaction concludes with the breakdown of the second transition state, the debinding of products, and possibly Mg^{2+} as well, and the return of the enzyme to its trypsin-sensitive, open conformation whereupon a new catalytic cycle can be initiated.

This description of the conformational dynamics of the H^+-ATPase molecule during its catalytic cycle is significantly different than the E1–E2 model for the P-type ATPases that is more commonly invoked [87]. The central feature of the E1–E2 model is a slow conformational interconversion between E1 and E2 states that changes the accessibility and affinity of the ion binding sites with respect to the membrane surface. In the E1 form, the ion-binding sites are of high affinity in contact with the cytoplasmic or ATP side of the membrane, and in the E2 form the sites are of low affinity in contact with the opposite side of the membrane. Phosphorylated forms participate in a similar interconversion between E1-P and E2-P. The forces that drive the conformational changes are rarely specified. Whereas this model may be convenient for making reference to approximate stages of the catalytic cycles of P-type ATPases generated by certain combinations of ions and other enzyme ligands, a major shortcoming of the E1–E2 model is that it fails to recognize the essential role of transition state binding affinity in the enzyme phosphorylation and dephosphorylation reactions as the real driving force for the conformational changes that occur during the catalytic cycles of these enzymes. Its heuristic value is therefore questionable. Moreover, the model has not withstood experimental scrutiny. In a trenchant biochemical analysis, Jencks and his colleagues have provided convincing evidence that the conformational transitions inherent in the E1–E2 model probably do not occur [reviewed in ref. 88]. Rather, the accessibility and affinity of the ion binding sites are controlled by the enzyme phosphorylation state, as implied here and explicitly proposed before [84, 89]. The E1–E2 model is thus not very useful and somewhat misleading, and should therefore be discarded. As a replacement, the simple scheme of Jencks [88] is appealing, supported by numerous experimental results and probably much closer to reality. It is also completely consistent with the conformational dynamics of the H^+-ATPase molecule described above.

Molecular mechanism of proton transport

The importance of the foregoing transition state considerations cannot be overemphasized, because they provide a rational explanation of the actual forces that drive the H^+-ATPase molecule and reactants through the various steps of the catalytic sequence. And an understanding of the driving forces is essential for a complete understanding of any molecular mechanism. However, although the above description may satisfactorily approximate the catalytic sequence with respect to the chemical transformations and major enzyme conformational changes involved in ATP hydrolysis catalyzed by the H^+-ATPase, and the forces that drive them, the question of the mechanism by which protons are translocated remains totally unresolved. By analogy with the Ca^{2+}-ATPase of sarcoplasmic reticulum, the ion binding site(s) of the H^+-ATPase are almost certainly in the transmembrane helix region [90, 91]. But

the means by which the enzyme phosphorylation and dephosphorylation reactions and associated conformational changes bring about the membrane side-specific ion binding site affinity and/or access changes necessary for the active transport of the proton(s) is presently unknown. The majority of the surface residues of the H^+-ATPase molecule that are occluded as a result of these ligand-induced conformational changes are probably present on the cytoplasmic side of the membrane, because this is the part of the molecule with by far the largest surface area, and because this is the side of the membrane from which the various ligands approach the catalytic center or active site. Thus, the act of cleft closure driven by transition state binding affinity provides a mechanism whereby proton binding residues normally in contact with the aqueous medium on the cytoplasmic side of the membrane can be isolated from it. And, if the same act of occlusion or any subsequent step in the catalytic cycle presents these residues to the aqueous medium the other side of the membrane, either directly or through a channel in the molecule, the prerequisites for gated, transmembrane proton movements have been met. This must be the way the ATPase accomplishes the access change required for a mediated transport mechanism and is especially pleasing because it invokes protein conformational dynamics that are already solidly established to exist. The most important question that remains then is the mechanism by which the ligand-induced interdomain movements are coupled with the proton-binding and release reactions. And the answer to this final essential question must await the availability of atomic resolution structures of the H^+-ATPase in the open conformation and one or more of its closed states.

1 Overton E. (1899) Ueber die allgemeinen osmotischen Eigenschaften der Zelle, ihre vermutlichen Ursachen und ihre Bedeutung für die Physiologie. Vierteljahrschr. Naturforsch. Ges. Zuerich **44:** 88–135
2 Jap B. K. and Walian P. J. (1996) Structure and functional mechanism of porins. Physiol. Rev. **76:** 1073–1088
3 Spudich J. L. (1998) Variations on a molecular switch: transport and sensory signalling by archaeal rhodopsins. Mol. Microbiol. **28:** 1051–1058
4 Reizer J. and Saier M. H. Jr (1997) Modular multidomain phosphoryl transfer proteins of bacteria. Curr. Opin. Struct. Biol. **7:** 407–415
5 Armstrong C. and Hille B. (1998) Voltage-gated ion channels and electrical excitability. Neuron **20:** 371–380
6 Gage P. W. (1998) Signal transmission in ligand-gated receptors. Immunol. Cell Biol. **76:** 436–440
7 Hamill O. P. and McBride D. W. Jr (1996) The pharmacology of mechanogated membrane ion channels. Pharmacol. Rev. **48:** 231–252
8 Verkman A. S., van Hoek A. N., Ma T., Frigeri A., Skach W. R., Mitra A. et al. (1996) Water transport across mammalian cell membranes. Am. J. Physiol. **270:** C12–30
9 Kumar N. M. and Gilula N. B. (1996) The gap junction communication channel. Cell **84:** 381–388
10 Trumpower B. L. and Gennis R. B. (1994) Energy transduction by cytochrome complexes in mitochondrial and bacterial respiration: the enzymology of coupling electron transfer reactions to transmembrane proton translocation. Annu. Rev. Biochem. **63:** 675–716
11 Pao S. S., Paulsen I. T. and Saier M. H. Jr (1998) Major facilitator superfamily. Microbiol. Mol. Biol. Rev. **62:** 1–34
12 Weber J. and Senior A. E. (1997) Catalytic mechanism of F1-ATPase. Biochim. Biophys. Acta **1319:** 19–58
13 Forgac M. (1998) Structure, function and regulation of the vacuolar (H^+)-ATPases. FEBS Lett. **440:** 258–263
14 Stangeland B., Fugslang A. T., Malmstrom S., Axelsen K. B., Baunsgaard L., Lanfermeijer F. C. et al. (1997) P-Type H^+- and Ca^{2+}-ATPases in plant cells. Ann. N. Y. Acad. Sci. **834:** 77–87
15 Schneider E. and Hunke S. (1998) ATP-binding-cassette (ABC) transport systems: functional and structural aspects of the ATP-hydrolyzing subunits/domains. FEMS Microbiol. Rev. **22:** 1–20
16 Henderson R., Baldwin J. M., Ceska T. A., Zemlin F., Beckmann E. and Downing K. H. (1990) Model for the structure of bacteriorhodopsin based on high-resolution electron cryo-microscopy. J. Mol. Biol. **213:** 899–929
17 Grigorieff N., Ceska T. A., Downing K. H., Baldwin J. M. and Henderson R. (1996) Electron-crystallographic refinement of the structure of bacteriorhodopsin. J. Mol. Biol. **259:** 393–421
18 Kimura Y., Vassylyev D. G., Miyazawa A., Kidera A., Matsushima M., Mitsuoka K. et al. (1997) Surface of bacteriorhodopsin revealed by high-resolution electron crystallography. Nature **389:** 206–211
19 Pebay-Peyroula E., Rummel G., Rosenbusch J. P. and Landau E. M. (1997) X-ray structure of bacteriorhodopsin at 2.5 Angstroms from microcrystals grown in lipidic cubic phases. Science **277:** 1676–1681
20 Luecke H., Richter H.-T. and Lanyi J. K. (1998) Proton transfer pathways in bacteriorhodopsin at 2.3 Angstrom resolution. Science **280:** 1934–1937
21 Weiss M. S. and Schulz G. E. (1992) Structure of porin refined at 1.8 Å resolution. J. Mol. Biol. **227:** 493–509
22 Cowan S. W., Schirmer T., Rummel G., Steiert M., Ghosh R., Pauptit R. A. et al. (1992) Crystal structures explain functional properties of two *E. coli* porins. Nature **358:** 727–733
23 Kreusch A. and Schulz G. E. (1994) Refined structure of the porin from *Rhodopseudomonas blastica*. Comparison with the porin from *Rhodobacter capsulatus*. J. Mol. Biol. **243:** 891–905
24 Schirmer T., Keller T. A., Wang Y. F. and Rosenbusch J. P. (1995) Structural basis for sugar translocation through maltoporin channels of 3.1 Å resolution. Science **267:** 512–514
25 Forst D., Welte W., Wacker T. and Diederichs K. (1998) Structure of the sucrose-specific porin ScrY from *Salmonella typhimurium* and its complex with sucrose. Nature Struct. Biol. **5:** 37–46
26 Locher K. P., Rees B., Koebnik R., Mitschler A., Moulinier L., Rosenbusch J. P. et al. (1998) Transmembrane signaling across the ligand-gated FhuA receptor: crystal structures of free and ferrichrome-bound states reveal allosteric changes. Cell **95:** 771–778
27 Buchanan S. K., Smith B. S., Venkatramani L., Xia D., Esser L., Palnitkar M. et al. (1999) Crystal structure of the outer membrane active transporter FepA from *Escherichia coli*. Nature Struct. Biol. **6:** 56–63
28 Iwata S., Ostermeier C., Ludwig B. and Michel H. (1995) Structure at 2.8 Å resolution of cytochrome c oxidase from *Paracoccus denitrificans*. Nature **376:** 660–669
29 Tsukihara T., Aoyama H., Yamashita E., Tomizaki T., Yamaguchi H., Shinzawa-Itoh K. et al. (1996) The whole structure of the 13-subunit oxidized cytochrome c oxidase at 2.8 Å. Science **272:** 1136–1144
30 Xia D., Yu C.-A., Kim H., Xia J.-Z., Kachurin A. M., Zhang L. et al. (1997) Crystal structure of the cytochrome bcl complex from bovine heart mitochondria. Science **277:** 60–66

31 Zhang Z., Huang L. S., Shulmeister V. M., Chi V. M., Kim K.-K., Hung L.-W. et al. (1998) Electron transfer by domain movement in cytochrome bc1. Nature **392:** 677–684

32 Abrahams J. P., Leslie A. G., Lutter R. and Walker J. E. (1994) Structure at 2.8 Å resolution of F1-ATPase from bovine heart mitochondria. Nature **370:** 621–628

33 Bianchet M. A., Hullihen J., Pedersen P. L. and Amzel L. M. (1998) The 2.8-Å structure of rat liver F1-ATPase: configuration of a critical intermediate in ATP synthesis/hydrolysis. Proc. Natl. Acad. Sci. USA **95:** 11065–11070

34 Doyle D. A., Cabral J. M., Pfuetzner R. A., Kuo A., Gulbis J. M., Cohen S. L. et al. (1998) The structure of the potassium channel: molecular basis of K^+-conduction and selectivity. Science **280:** 69–77

35 Chang G., Spencer R. H., Lee A. T., Barclay M. T. and Rees D. C. (1998) Structure of the MscL homolog from *Mycobacterium tuberculosis*: a gated mechanosensitive ion channel. Science **282:** 2220–2226

36 Pedersen P. L. and Carafoli E. (1987) Ion motive ATPases. I. Ubiquity, properties and significance to cell function. Trends Biochem. Sci. **12:** 146–150

37 Slayman C. L. (1965) Electrical properties of *Neurospora crassa*. Effects of external cations on the intracellular potential. J. Gen. Physiol. **49:** 69–92

38 Slayman C. L. (1970) Movement of ions and electrogenesis in microorganisms. Am. Zool. **10:** 377–392

39 Scarborough G. A. (1975) Isolation and characterization of *Neurospora crassa* plasma membranes. J. Biol. Chem. **250:** 1106–1111

40 Scarborough G. A. (1977) Properties of the *Neurospora crassa* plasma membrane ATPase. Arch. Biochem. Biophys. **180:** 384–393

41 Scarborough G. A. (1976) The *Neurospora* plasma membrane ATPase is an electrogenic pump. Proc. Nat. Acad. Sci. USA **73:** 1485–1488

42 Scarborough G. A. (1980) Proton translocation catalyzed by the electrogenic ATPase in the plasma membrane of *Neurospora*. Biochemistry **19:** 2925–2931

43 Dame J. B. and Scarborough G. A. (1980) Identification of the hydrolytic moiety of the *Neurospora* plasma membrane H^+-ATPase and demonstration of a phosphoryl-enzyme intermediate in its catalytic mechanism. Biochemistry **19:** 2931–2937

44 Dame J. B. and Scarborough G. A. (1981) Identification of the phosphorylated intermediate of the *Neurospora* plasma membrane H^+-ATPase as beta-aspartyl phosphate. J. Biol. Chem. **256:** 10724–10730

45 Addison R. and Scarborough G. A. (1981) Solubilization and purification of the *Neurospora* plasma membrane H^+-ATPase. J. Biol. Chem. **256:** 13165–13171

46 Smith R. and Scarborough G. A. (1984) Large-scale isolation of the *Neurospora* plasma membrane H^+-ATPase. Anal. Biochem. **138:** 156–163

47 Scarborough G. A. (1988) Large-scale purification of the plasma membrane H^+-ATPase from a cell wall-less mutant of *Neurospora crassa*. Methods Enzymol. **157:** 574–579

48 Scarborough G. A. and Addison R. (1984) On the subunit composition of the *Neurospora* plasma membrane H^+-ATPase. J. Biol. Chem. **259:** 9109–9114

49 Goormaghtigh E., Chadwick C. and Scarborough G. A. (1986) Monomers of the *Neurospora* plasma membrane H^+-ATPase catalyze efficient proton translocation. J. Biol. Chem. **261:** 7466–7471

50 Mahanty S. K., Rao U. S., Nicholas R. A. and Scarborough G. A. (1994) High-yield expression of the *Neurospora crassa* plasma membrane H^+-ATPase in *Saccharomyces cerevisiae*. J. Biol. Chem. **269:** 17705–17712

51 Chadwick C., Goormaghtigh E. and Scarborough G. A. (1987) A hexameric form of the *Neurospora* crassa plasma membrane H^+-ATPase. Arch. Biochem. Biophys. **252:** 348–356

52 Hennessey J. P. Jr and Scarborough G. A. (1988) Secondary structure of the *Neurospora crassa* plasma membrane H^+-ATPase as estimated by circular dichroism. J. Biol. Chem. **263:** 3123–3130

53 Goormaghtigh E., Vigneron L., Scarborough G. A. and Ruysschaert J.-M. (1994) Tertiary conformational changes of the *Neurospora crassa* plasma membrane H^+-ATPase monitored by hydrogen/deuterium exchange kinetics: a Fourier transform infrared spectroscopy approach. J. Biol. Chem. **269:** 27409–27413

54 Rao U. S., Hennessey J. P. Jr and Scarborough G. A. (1988) Protein chemistry of the *Neurospora crassa* plasma membrane H^+-ATPase. Anal. Biochem. **173:** 251–264

55 Hennessey J. P. Jr and Scarborough G. A. (1989) An optimized procedure for SDS-PAGE analysis of hydrophobic peptides from an integral membrane protein. Anal. Biochem. **176:** 284–289

56 Hennessey J. P. Jr and Scarborough G. A. (1990) Direct evidence for the cytoplasmic location of the NH_2- and COOH-terminal ends of the *Neurospora crassa* plasma membrane H^+-ATPase. J. Biol. Chem. **265:** 532–537

57 Scarborough G. A. and Hennessey J. P. Jr (1990) Identification of the major cytoplasmic regions of the *Neurospora crassa* plasma membrane H^+-ATPase using protein chemical techniques. J. Biol. Chem. **265:** 16145–16149

58 Rao U. S., Hennessey J. P. Jr and Scarborough G. A. (1991) Identification of the membrane-embedded regions of the *Neurospora crassa* plasma membrane H^+-ATPase. J. Biol. Chem. **266:** 14740–14746

59 Rao U. S., Bauzon D. D. and Scarborough G. A. (1992) Cytoplasmic location of amino acids 359–440 of the *Neurospora crassa* plasma membrane H^+-ATPase. Biochim. Biophys. Acta **1108:** 153–158

60 Rao U. S. and Scarborough G. A. (1990) Chemical state of the cysteine residues in the *Neurospora crassa* plasma membrane H^+-ATPase. J. Biol. Chem. **265:** 7227–7235

61 Goffeau A. and Slayman C. W. (1981) The proton-translocating ATPase of the fungal plasma membrane. Biochim. Biophys. Acta **639:** 197–223

62 Nakamoto R. K. and Slayman C. W. (1989) Molecular properties of the fungal plasma-membrane H^+-ATPase. J. Bioenerg. Biomemb. **21:** 621–632

63 Serrano R. (1989) Structure and function of plasma membrane ATPase. Annu. Rev. Plant. Physiol. Plant Mol. Biol. **40:** 61–94

64 Scarborough G. A. (1992) The *Neurospora crassa* plasma membrane H^+-ATPase. In: Molecular Aspects of Membrane Proteins, pp. 117–134, de Pont J. J. H. H. M. (ed.), Elsevier, Amsterdam

65 Scarborough G. A. (1996) The *Neurospora* plasma membrane proton pump. In: Handbook of Biological Physics, Transport Processes in Eukaryotic and Prokaryotic Organisms, vol. 2, pp. 75–92, Konings W. N., Kaback H. R. and Lolkema J. S. (eds), Elsevier Science, Amsterdam

66 Rao R. and Slayman C. W. (1996) Plasma membrane and related ATPases. In: The Mycota, Biochemistry and Molecular Biology, vol. 3, pp. 30–56, Brambl R. M. and Marzluf G. A. (eds), Springer, Berlin

67 Scarborough G. A. (1994) Large single crystals of the *Neurospora crassa* plasma membrane H^+-ATPase: an approach to the crystallization of integral membrane proteins. Acta Cryst. D **50:** 643–649

68 McPherson A. (1982) Preparation and Analysis of Protein Crystals, Wiley, New York

69 Cyrklaff M., Auer M., Kühlbrandt W. and Scarborough G. A. (1995) 2D structure of the *Neurospora crassa* plasma membrane ATPase as determined by electron cryomicroscopy. EMBO J. **14:** 1854–1857

70 Hasler L., Heymann J. B., Engel A., Kistler J. and Walz T. (1998) 2D crystallization of membrane proteins: rationales and examples. J. Struct. Biol. **121:** 162–171

71 Auer M., Scarborough G. A. and Kühlbrandt W. (1999) Surface crystallization of the plasma membrane H^+-ATPase on a carbon support film for electron crystallography. J. Mol. Biol. **287:** 961–968

72 Auer M., Scarborough G. A. and Kühlbrandt W. (1998) Three-dimensional map of the plasma membrane H^+-ATPase in the open conformation. Nature **392:** 840–843
73 Song L. and Gouaux J. E. (1997) Membrane protein crystallization: application of sparse matrices to the α-hemolysin heptamer. Methods Enzymol. **276:** 60–74
74 Addison R. and Scarborough G. A. (1982) Conformational changes of the *Neurospora* plasma membrane H^+-ATPase during its catalytic cycle. J. Biol. Chem. **257:** 10421–10426
75 Mildvan A. S. (1979) The role of metals in enzyme-catalyzed substitutions at each of the phosphorus atoms of ATP. Adv. Enzymol. **49:** 103–126
76 Knowles J. R. (1980) Enzyme-catalyzed phosphoryl transfer reactions. Annu. Rev. Biochem. **49:** 877–919
77 Pauling L. (1946) Molecular architecture and biological reactions. Chem. Eng. News **24:** 1375–1377
78 Jencks W. P. (1966) Strain and conformation change in enzymatic catalysis. In: Current Aspects of Biochemical Energetics, pp. 273–298, Kaplan N. O. and Kennedy E. P. (eds), Academic Press, New York
79 Wolfenden R. (1969) Transition state analogues for enzyme catalysis. Nature **223:** 704–705
80 Lienhard G. (1973) Enzymatic catalysis and transition-state theory. Science **180:** 149–154
81 Fersht A. R., Leatherbarrow R. J. and Wells T. N. C. (1986) Binding energy and catalysis: a lesson from protein engineering of the tyrosyl-tRNA synthetase. Trends Biochem. Sci. **11:** 321–325
82 Frost A. A. and Pearson R. G. (1961) Transition-state theory. In: Kinetics and Mechanism, 2nd edn, pp. 77–102, Wiley, New York
83 Macara I. G. (1980) Vanadium-an element in search of a role. Trends Biochem. Sci. **5:** 92–94
84 Scarborough G. A. (1985) Binding energy, conformational change, and the mechanism of transmembrane solute movements. Microbiol. Rev. **49:** 214–231
85 Mao B., Pear M. R., McCammon J. A. and Quiocho F. A. (1982) Hinge-bending in L-arabinose-binding protein: the Venus's-flytrap model. J. Biol. Chem. **257:** 1131–1133
86 Mandala S. M. and Slayman C. W. (1988) Identification of tryptic cleavage sites for two conformational states of the *Neurospora* plasma membrane H^+-ATPase. J. Biol. Chem. **263:** 15122–15128
87 Inesi G. (1985) Mechanism of calcium transport. Annu. Rev. Physiol. **47:** 573–601
88 Jencks W. P. (1989) How does a calcium pump pump calcium? J. Biol. Chem. **264:** 18855–18858
89 Scarborough G. A. (1982) Chemiosmotic models for the mechanisms of the cationmotive ATPases. Ann. N. Y. Acad. Sci. **402:** 99–115
90 Scott T. L. (1988) Molecular topography of the Ca^{++}-ATPase of sarcoplasmic reticulum. Mol. Cell. Biochem. **82:** 51–54
91 Clarke D. M., Loo T. W., Inesi G. and MacLennan D. H. (1989) Location of high affinity Ca^{++}-binding sites within the predicted transmembrane domain of the sarcoplasmic reticulum Ca^{++}-ATPase. Nature **339:** 476–478